

STUDY OF VERY SHORT GAMMA-RAY BURSTS

David B. Cline, Christina Matthey, and Stanislaw Otwinowski

University of California, Los Angeles

Department of Physics and Astronomy, Box 951457

Los Angeles, CA 90095-1547 USA

UCLA-APH-0106-4/99

Received _____; accepted _____

ABSTRACT

We have carried out a detailed study of the morphology of gamma-ray bursts (GRBs) with time duration less than 100 ms that includes: (1) a fast-Fourier spectrum analysis, (2) a comparison with the Stern analysis of longer bursts, (3) an inner comparison of the properties of the short bursts, and (4) a comparison of the short burst properties with the bulk of the GRBs from the Burst and Transient Source Experiment (BATSE) 4B catalogue. We have used the time tagged event (TTE) BATSE 3B data, which is available to the public, for part of the analysis. We show that these bursts are very different from the rest of the GRB events. The short bursts appear to be nearly identical, suggesting a separate class of GRBs. We also show that the short bursts have a Euclidean space–time distribution, in sharp contrast to the longer bursts with $\tau_{\text{duration}} > 100$ ms that implies that these sources are likely local. Finally we compare the bursts with a model of primordial black hole (PBH) evaporation at the quark–gluon (Q–G) phase transition temperature and other shock wave models.

1. INTRODUCTION

The physical origin of gamma-ray bursts (GRBs) continues to be unknown. It is clear that the predominate fraction of the GRBs with $t > 1$ s have a nearly chaotic luminosity time behaviour and the events are well described by the Stern time analysis (Stern 1996). It is very likely that these GRBs are from cosmological sources. For some time, there has been evidence for at least two classes of GRBs, with a separation time duration of ~ 1 s or perhaps less (Kouveliotou et al. 1993). In a report (Cline, Sanders, & Hong 1997), we reported on our studies of 12 GRBs from the Burst and Transient Source Experiment (BATSE) 3B catalogue (Meegan et al. 1996) in an attempt to find some regularity. We have used the BATSE time tagged event (TTE) data in this analysis and performed a fast-Fourier analysis in these time profiles (Cline, Matthey, & Otwinowsky 1998a). Our general conclusion is that the shortest of these events (with a duration of < 100 ms) behave almost identically, unlike the bulk of the GRBs, which possibly indicates a different physical origin from that of the longer GRBs. We also compare these event distributions with the bulk of the GRBs to show, by contrast, the great differences in the various sources of the GRB samples. We briefly explore one such origin, namely, that these GRBs arrive from a fireball resulting from a primordial black hole (PBH) at the quark–gluon (Q–G) phase transition that could give rise to such a class of events in Section 8.

The plan of this paper is to first describe the characteristics of the short GRBs – we study the TTE data for the BATSE 3B catalogue for a detailed fit of the time profile and then to discuss various analyses of the events including a fast-Fourier transform analysis and the resulting power spectrum density (PSD). Next we discuss some of the problems of getting such short bursts from current cosmological fireball models. We then discuss one model that could give such bursts from PBH evaporation. Finally, using the BATSE 4B catalogue, we compare the $\ln N$ – $\ln S$ distributions of the short GRBs with the bulk of the

GRBs where we use a hardness cut to separate the data into different classes of events.

2. EVENT SELECTION USING BATSE 3B TTE DATA

We have studied all events with T_{90} less than 200 ms and then refit the time profile using the TTE data with the BATSE data set (we restrict this part of the analysis to BATSE 3B data), BATSE 3B catalogue (see Meegan et al. 1996). We found 12 events that have a TTE fitted time duration of less than 100 ms. These events are listed in Table 1 with the fitted time duration. We then closely inspected the 12 events and found that some have additional structure. Of the 10 good/fair events, 9 have a time duration of 90 ms or less. Our goal is to select a similar class of events for study, which constitutes the bulk of the short bursts. We only study single peak events, which are the bulk of the short bursts. As we will show, these events appear to be almost identical in all features, except for BATSE trigger 2463, which we delete in this analysis. This event has a clearly different energy spectrum from the bulk of the short GRB events. This sample constitutes the set of events studied here. We show the time profiles in different photon energy bins in Figure 1.

3. FOURIER TRANSFORM AND THE POWER SPECTRUM DENSITY

We have carried out a fast-Fourier transform of all events with T_{90} duration of less than 200 ms. We report here the study of the PSD for the eight events with time duration of less than 66 ms (see Figure 2) discussed above. Note the remarkable similarity of the PSDs for these events.

In the general study of all GRBs, there has never been any evidence of two bursts being alike. In fact, the nature of the GRB source is likely to give a chaotic behaviour. However for the eight events in the sample reported here, there is clear evidence for a high

frequency component in the PSD spectrum.

4. COMPARISON WITH THE STERN ANALYSIS

While there are no exact models for any GRBs, there have been some successful phenomenological models that fit the time distribution on average. One such analysis was carried out by B.E. Stern (1996). In this model the GRBs are assumed to fit an analytical model after the first peak of the GRB:

$$I \sim e^{-(t/t_0)^{1/3}} \quad , \quad (1)$$

where t is the time after the peak and t_0 is a constant. Stern showed that the GRBs with duration greater than about 250 ms fit this distribution very well. In a model-dependent way, one can associate this behaviour as a sort of cooling-off phase after the initial burst, which seems also to be the case for solar flares (although with a different t_0 constant). As far as we know, this is the most successful analytical description of the general GRB time profiles. The results of our analysis of the sum¹ of all 12 short bursts (see Table 1) using the analytical form (1) are shown in Figure 3. The t_0 value obtained from the fit (0.0016 ± 0.0007 s) is far from the value (between 0.3 s and 1.0 s) found by Stern and the fit ($\chi^2/\text{ndf}=770/219$) is not good. The failure of the Stern function fit (χ^2 of 770 for 219 degrees of freedom) indicates that the short GRBs have a quantitatively different shape from the long GRBs. In essence, the short GRBs are much more symmetric in the rise and fall of the pulse than are the long GRBs. We believe that this is an indication that these very short bursts are a different class of phenomena from the bulk of the GRBs.

¹In the sum, events are shifted to put the maxima at the same time.

Table 1. EVENT SELECTION AND PROPERTIES (BATSE 3B)

Trigger Number	Duration from TTE Fit (s)	Hardness Ratio	Comments	Used in This Analysis
01453	0.006 ± 0.0002	6.68 ± 0.33	Poor event, precursor	No
00512	0.014 ± 0.0006	6.07 ± 1.34	Good event	Yes
01649	0.020 ± 0.0080		Fair event*	Yes
00207	0.030 ± 0.0019	6.88 ± 1.93	Good event	
02615	0.034 ± 0.0032	5.42 ± 1.15	Good event	Yes
03173	0.041 ± 0.0020	5.35 ± 0.27	Poor event, precursor	No
02463	0.049 ± 0.0045	1.60 ± 1.55	Good event	No
00432	0.050 ± 0.0018	7.46 ± 1.17	Good event	Yes
00480	0.062 ± 0.0020	7.14 ± 0.96	Good event	Yes
03037	0.066 ± 0.0072	4.81 ± 0.98	Good event	Yes
02132	0.090 ± 0.0081	3.64 ± 0.66	Good event	Yes
00799	0.097 ± 0.0101	2.47 ± 0.39	Fair event*	No

*Fair event, small additive structure

5. COMPARISON OF THE PROPERTIES OF THE EVENTS

As far as we can tell, no two long duration bursts are alike. We find that this is not true for the very short bursts, which seem to be identical except for a factor of two in time duration. We illustrate this in Figure 1, which shows the time distribution, without the lowest (< 50 keV) energy, for the eight very short bursts selected from the BATSE 3B TTE data, and in Figure 4, which shows the energy distribution of eight short bursts. We include this plot that shows that the energy distributions as well as the hardness are nearly identical for these events. This fact can also be learned from the hardness values in Table 1 (Cline et al. 1997). Within error, all have the same hardness (excluding BATSE trigger 2463). To our knowledge there is no evidence for any other set of GRBs with such identical features. We believe that this indicates a simple and identical production process for this class of events.

6. DETECTION EFFICIENCY FOR SHORT BURSTS

The bulk of the very short bursts identified here all have time duration at or below the BATSE 64-ms integration time. We therefore believe that the BATSE trigger is likely an inefficient method of identifying such events; we also believe that many weak bursts may have been missed.

Recently the issue of detecting short GRBs with time duration of $\tau < 64$ ms (the smallest BATSE trigger time scale) has been raised (Nemiroff et al. 1998). They show that the detector efficiency will drop sharply for bursts below 64 ms. Since several GRBs have been detected with bursts less than 64 ms, it is likely that there is a significant population of short bursts that have been missed. Here we will not attempt to determine the detector efficiency as a function of τ but simply refer to the work of Nemiroff et al. (1998). They

state that there could be as many missed GRBs of 1-ms duration as the number that have been detected at 10 s.

Since the detection of the short bursts is uncertain, we may not expect as clear a separation of this class of events from the bulk of the GRBs as from the two classes of GRBs that have been identified (Kouveliotou et al. 1993).

7. BEHAVIOUR OF INDIVIDUAL EVENTS

7.1. BATSE Trigger Number 512

To obtain a better understanding of the short bursts, we discuss three individual bursts that have more detailed information than the bulk of the events. According to the arguments given above, we expect all of the short bursts to be very similar and, therefore, we assume that the behaviour of these special bursts is likely an example for all short bursts. If these events are typical of the short bursts, then we can see a clear behaviour in the fine time structure and the detected gamma energy distribution. We start with the incredible GRB trigger 512. In Figures 5 and 6, we note the detailed fine structure for BATSE trigger 512, which has the finest time structure of any GRB observed to date – possibly down to $20 \mu\text{s}$ level. This was a very bright burst and allowed unpredicted time information.

7.2. PHEBUS Event Numbers PB900320 and PB900813

The PHEBUS GRB detector [see PHEBUS catalogue (Terekov et al. 1994)], has recorded two very interesting short time events, shown in Figure 7. As far as can be determined, these events are identical (note that the energy distribution are fit to a synchrotron and are identical). Because of a thicker absorber, the PHEBUS detector has a

larger energy-range capacity than that of the BATSE detector.

Thus this detector can record photon energies up to 180 MeV in contrast to BATSE, which is only sensitive up to about 580 keV due to the the absorbers. Note that these two PHEBUS events have photon energies above 1 MeV. Thus the short GRBs have energetic photons in the spectrum.

8. EXPECTATIONS FOR SUBSTRUCTURE IN FIREBALL MODELS

As we have shown, the very short bursts analyzed here have strong substructure on the scale of 50 μ s in at least one case and pulse rise times of the order of milliseconds. We now explore the models for GRBs of cosmological origin. For the fireball models with total energy release of 10^{51} ergs, it is very difficult to get such short bursts, because it requires very large Lorentz boosts for the shock front. In these same models, the possibility of temporal substructure has been studied recently by Panaitescu and Mészáros (1998) and they found that it describes the important characteristics of the bulk of the GRBs in the BATSE sample rather well.

In one fireball model, the burst time scale is set by the hydrodynamic time scale t_{dec} and the fireball Lorentz factor is $\Gamma_0 = E_0/Mc^2$, where E_0 is the total energy released and M is the entire baryonic mass in the fireball, which gives $T = 10 \cdot t_{\text{dec}}/2 \cdot \Gamma_0^2$. The BATSE data can be explained by Γ_0 values of ~ 100 – 500 , and $E_0 \sim 10^{50}$ erg gives $T \sim 2$ – 20 s to get very short bursts requiring a very large value of Γ_0 . For temporal substructure to occur, it must be related to even larger values of Γ_0 and other factors that we will not discuss here. In the case of BATSE trigger 512 with $\Delta t \sim 50 \mu$ s, the Lorentz factor must be extremely high (50,000), which seems to be very unphysical in this model. This model also predicts very asymmetric rise and fall times for the bursts that are very similar to those

of the Stern analysis discussed before. As we have shown, the very short bursts are rather symmetric. We conclude that it is unlikely that the very short bursts can be described by a cosmological fireball model.

We also consider the effects of internal shocks, as has been discussed recently by Kobayashi, Piran, and Sari (1997) and references included therein. In this model, the source releases energy of 10^{52} erg with negligible baryonic contamination $\leq 10^{-5}M_{\odot}$. The region of GRB emission is found to be $\sim 10^{11}$ cm and fireball shells collide with distances of $\sim 10^{14}$ cm, generating the internal shocks and the time variation in the GRB. The natural times for such GRBs are $r/\Gamma_0^2c \sim 10^{14}/(10^2 \times 3 \times 10^{10}) \sim 30$ s, which are far beyond the time scale of the short bursts studied here. The time scale of the internal shocks is $\sim 10^{11}/\Gamma_0^2c \geq 3$ ms, which is far longer than the $50 \mu\text{s}$ structure observed for BATSE trigger 512. We conclude that cosmological fireball models with internal shocks are unlikely to produce events of the type studied here. The main reason is that the enormous energy released requires a large volume for photon emissions, which implies longer time scales for the overall burst and variation. We therefore conclude that it is very unlikely that these GRBs are due to cosmological sources.

9. ONE POSSIBLE MODEL FOR THE ORIGIN OF THE VERY SHORT BURSTS

Ever since the discussion of PBHs began, there have been suggestions for the experimental detection of such objects. However, the real-time detection depends on the final state evolution of the PHB; as it sheds mass, the temperature of the PHB rises into the region of hadronic interactions and hadronic final states. The most extreme model used to simulate this final state was the Hagedorn model, which predicted an explosion lasting $\sim 10^{-7}$ s, whereas other QCD-inspired calculations suggested a final-state collapse time of

the order of seconds. We questioned the validity of the QCD-inspired calculations, pointing out that final state interactions and non-perturbation effects could increase the low-energy particle luminosity and even the collapse time, both of which would make detection easier. We note that there are already indications of two classes of GRBs (Kouveliotou et al. 1993). The approach taken here is to determinate if there are GRBs that could be consistent with PBH evaporation, not to attempt to prove the existence of PBHs at this stage. Hawking (1974) showed that the temperature of the PHB increases as it loses mass during its lifetime. Mass, in the context of the standard model of particle physics, is lost at a rate

$$\frac{dM}{dt} = -\frac{\alpha(M)}{M^2} , \quad (2)$$

where $\alpha(M)$, the running constant, counts the particle degree of freedom in the PBH evaporation. The value of the $\alpha(M)$ is model dependent (Cline et al. 1997; Hawking 1974).

Black holes at the evaporation state in the present epoch can be calculated as

$$M_* \simeq [3\alpha(M_*)\tau_{\text{evap}}]^{1/3} \simeq 7.0 \times 10^{14} \text{g} , \quad (3)$$

where $\alpha(M_*) \simeq 1.4 \times 10^{-3}$. Thus, the number of black holes with critical mass M_* in their final state of evaporation is

$$\frac{dn}{dt} = \frac{3\alpha(M_*)}{M_*^3} N = 2.2 \times 10^{-10} N \text{pc}^{-3} \text{y}^{-1} , \quad (4)$$

where N is the number of PBHs per pc^{-3} in the Galaxy.

In previous works (Cline & Hong 1992; Cline et al. 1997) it was shown that short GRBs have the characteristics expected for PBH evaporation. In these same references, it has been shown that the Hawking Radiation can be detected as a short GRB from PBHs as far away as a few parsec, because of the enhancement from the quark–gluon phase transition, provided it is a first order transition. In this case, and using constraints on the PBH density universe in these references, we would expect a few events per year to be detected by BATSE. This rate is consistent with the rate of short GRBs studied in this paper.

10. COMPARISON WITH OTHER GRBs

We classify all GRBs into three different categories: one with $\tau > 1$ s (long, L), one with $1 \text{ s} > \tau > 0.1 \text{ s}$ (medium, M), and one with $\tau \leq 100$ ms (short, S), which is the focus of this investigation. The location of these events is shown in Figure 8. In Figure 9 we show the contrast between the S and M classes of events, which appears to be counter intuitive.

We note that the short bursts are strongly consistent with a $C_p^{-3/2}$ spectrum, indicating a Euclidean source distribution, as was shown previously by (D. Cline et al. 1997). In the medium (100 ms to 1 s) time duration, the $\ln N$ – $\ln S$ distribution seems to be non-Euclidean; in the long duration ($\tau > 1$ s) bursts, the situation is more complicated as we have shown recently (Cline, Matthey, & Otwinowski 1998b). The $\langle V/V_{\max} \rangle$ for the S, M, and L class of events is, respectively, 0.52 ± 0.1 , 0.36 ± 0.02 , 0.31 ± 0.01 . (In this case, we have used the BATSE 5B data² to obtain the best statistics.)

We point out again that the 12 events discussed in Sections 2, 3, and 4 are obtained from the short GRBs in the BATSE 3B catalogue, as explained in Section 2; the larger sample of short GRBs used in Section 10 came from the most recent data up to Nov. 18, 1998 (beyond the BATSE 4B catalogue). In the latter case, we needed to collect the largest statistics for the results in Figure 9.

One possibility for explaining these effects is that the distribution of the short bursts may come from a local Galactic source. This explanation is not viable for the medium time bursts, since $\langle V/V_{\max} \rangle$ is 0.36 ± 0.02 , indicating a likely cosmological source. The longer bursts are clearly from cosmological distance.

By studying Figures 1–3, it can be seen that these events could well be nearly identical

²We understand BATSE 5B data to include all BATSE data registered before Nov. 18, 1998.

except for different time durations, and the identical energy spectra for the two PHEBUS events (Figure 7) gives additional support. In addition, the $\ln N$ – $\ln S$ behaviour (Figures 8 and 9) suggests an extremely compact source. These are all consistent with PBH evaporation as the source of GRBs and imply a Galactic origin of the short GRBs. Of course there could be other types of Galactic sources as well.

In summary, we have shown that the GRBs with $\tau < 100$ ms likely are due to a separate class of sources and appear to be nearly identical in contrast to the bulk of GRBs. In this analysis, we have studied a small class of BATSE 3B TTE data in detail, and to improve the statistical power for some issues, we have used BATSE 4B and the latest BATSE 5B data. We do not believe this study warrants the use of the full TTE data for BATSE 4B or BATSE 5B, since the point is to show a general morphology of the GRBs, not a complete statistical analysis at this stage. It is likely that the source is local or Galactic, in contrast to the cosmological origin of the bulk of GRBs. One model source that may produce such a unique class of GRBs is the evaporation of PBHs. Independent of that model, we believe these short bursts constitute a third class of GRBs.

11. Acknowledgment

We wish to thank members of the BATSE team for discussions, especially J. Norris and G. Fishman.

REFERENCES

- Cline, D. B., & Hong, W. P. 1992, *ApJ*, 401, L57
- Cline, D. B., Sanders, D. A., & Hong, W. 1997, *ApJ*, 486, 169
- Cline, D. B., Matthey, C., & Otwinowski, S. 1998, in *Proc. 4th Huntsville Symp* 438 (New York: AIP)
- Cline, D. B., Matthey, C., & Otwinowski, S. 1998 *Proc. 14th IAP Colloq*, in press
- Hawking, S. W. 1974, *Nature*, 30, 248
- Kobayashi, S., Piran, T., & Sari, R. 1997, *ApJ*, 490, 92
- Kouveliotou, C., et al. 1993, *ApJ*, 413, L101
- Meegan, C. A., et al. 1996, *ApJS*, 106, 65
- Nemiroff, R. J. Norris, J. P., Bonnell, J. T., & Marani, G. F. 1998 *ApJ*, 494, L137
- Panaitescu, A., & Mészáros, P. 1998, *ApJ*, 492, 683
- Terekhov, O. V., et al. 1994, *Astron. Lett.*, 265, 20
- Stern, B. E. 1996, *ApJ*, 464, L111

Figure Captions:

Fig. 1.— Time profile for the eight short GRBs in different energy bins from the BATSE 3B TTE data.

Fig. 2.— The power spectrum density of eight short GRBs using BATSE 3B TTE data.

Fig. 3.— The result of applying the statistical Stern analysis to the sum of 12 short GRBs.

Fig. 4.— The energy spectrum of the eight events discussed in the text plotted as a function of time.

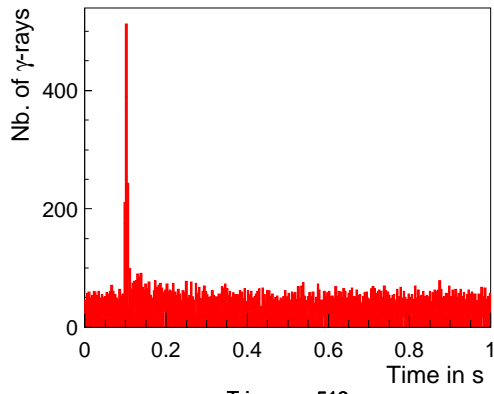
Fig. 5.— Plot of the rise time structure for GRB trigger number 512.

Fig. 6.— Plot of the fine time structure for GRB trigger number 512.

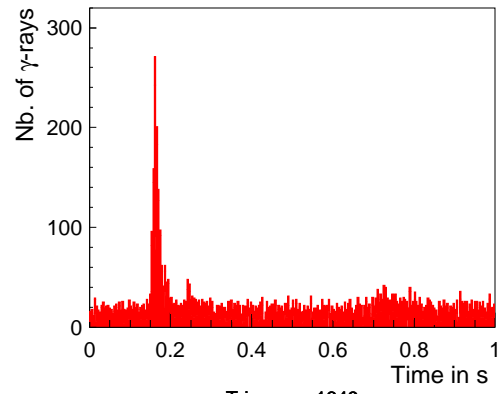
Fig. 7.— Two short bursts from the PHEBUS detector: Time profiles of (a) PB900813 and (b) PB900320, and energy spectrum of (c) PB900813 and (d) PB900320.

Fig. 8.— Hardness (H) vs duration (S = short, M = medium) of BATSE-4B GRBs.

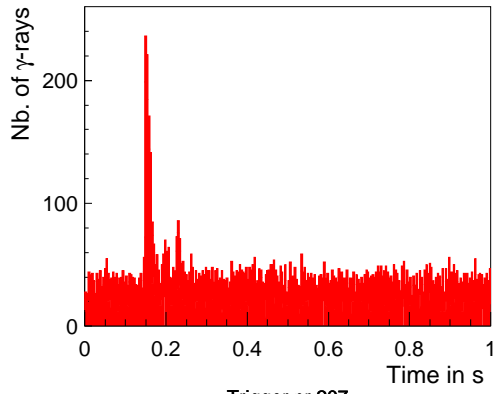
Fig. 9.— Comparison of the $\ln N$ – $\ln S$ distribution of the short (S) and medium (M) GRBs for BATSE 4B data.



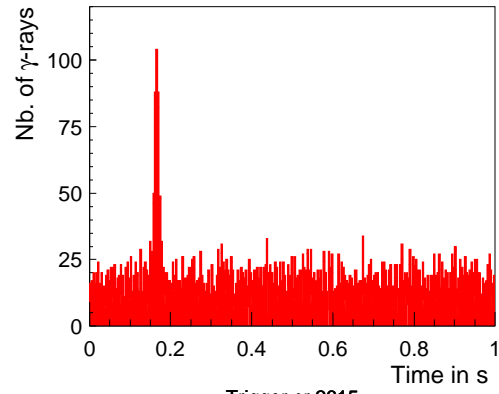
Trigger nr 512



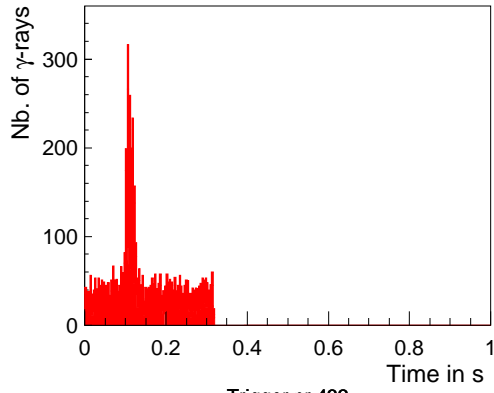
Trigger nr 1649



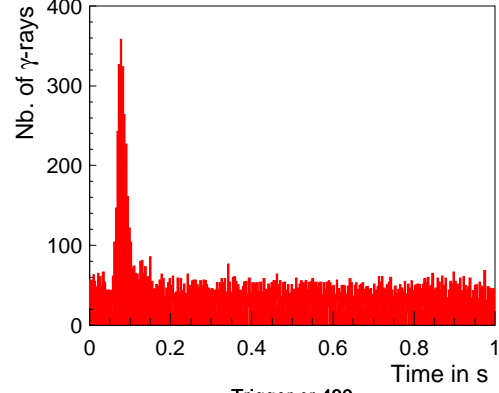
Trigger nr 207



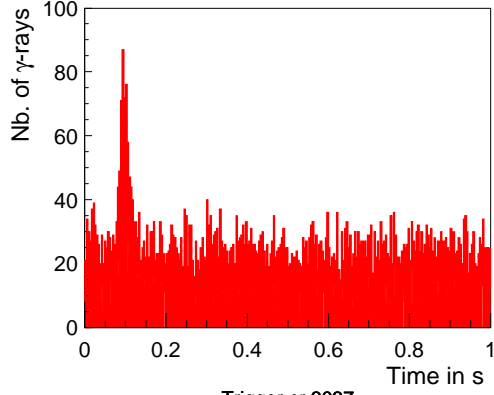
Trigger nr 2615



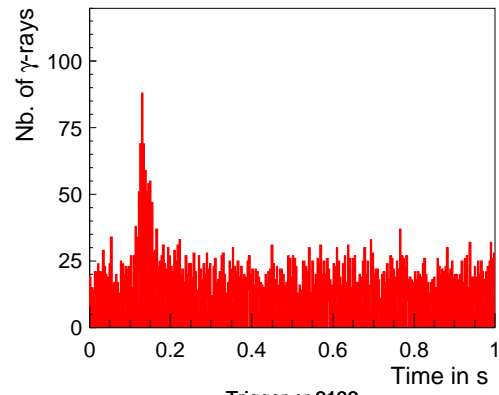
Trigger nr 432



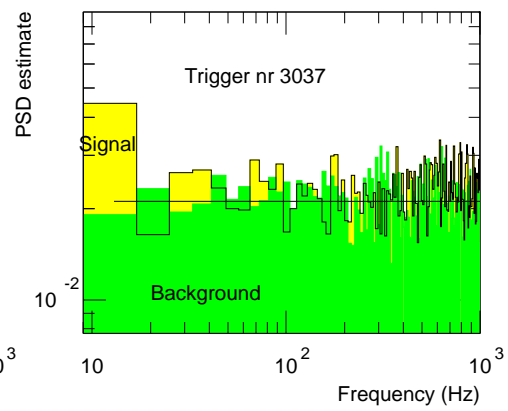
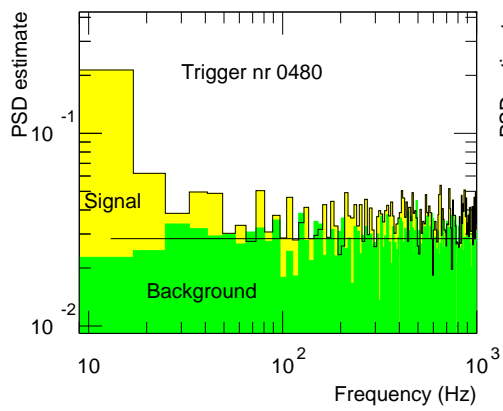
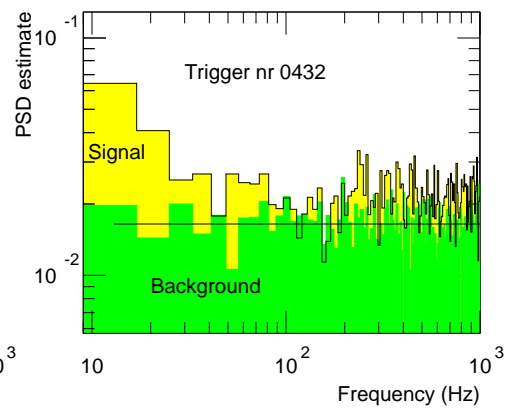
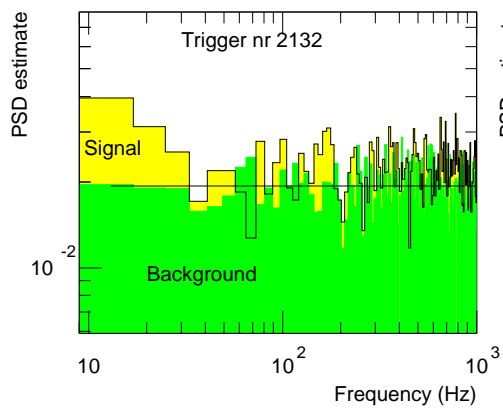
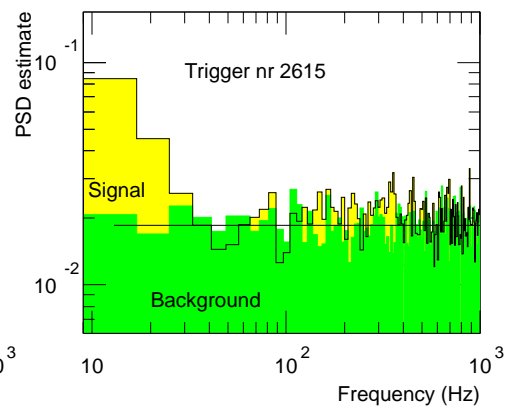
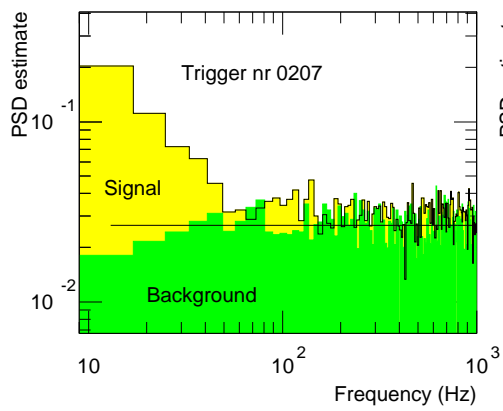
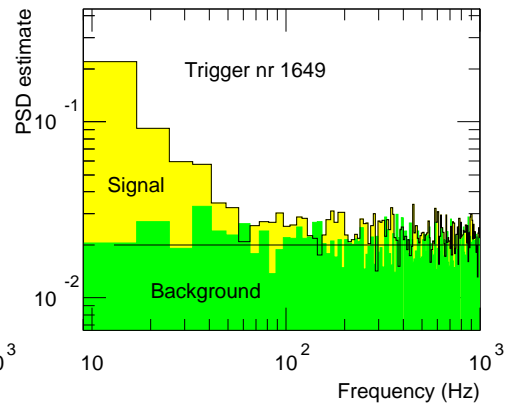
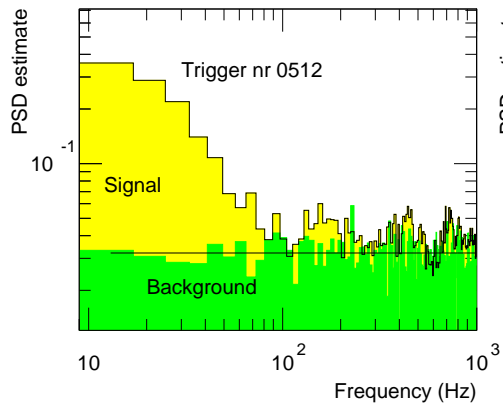
Trigger nr 480

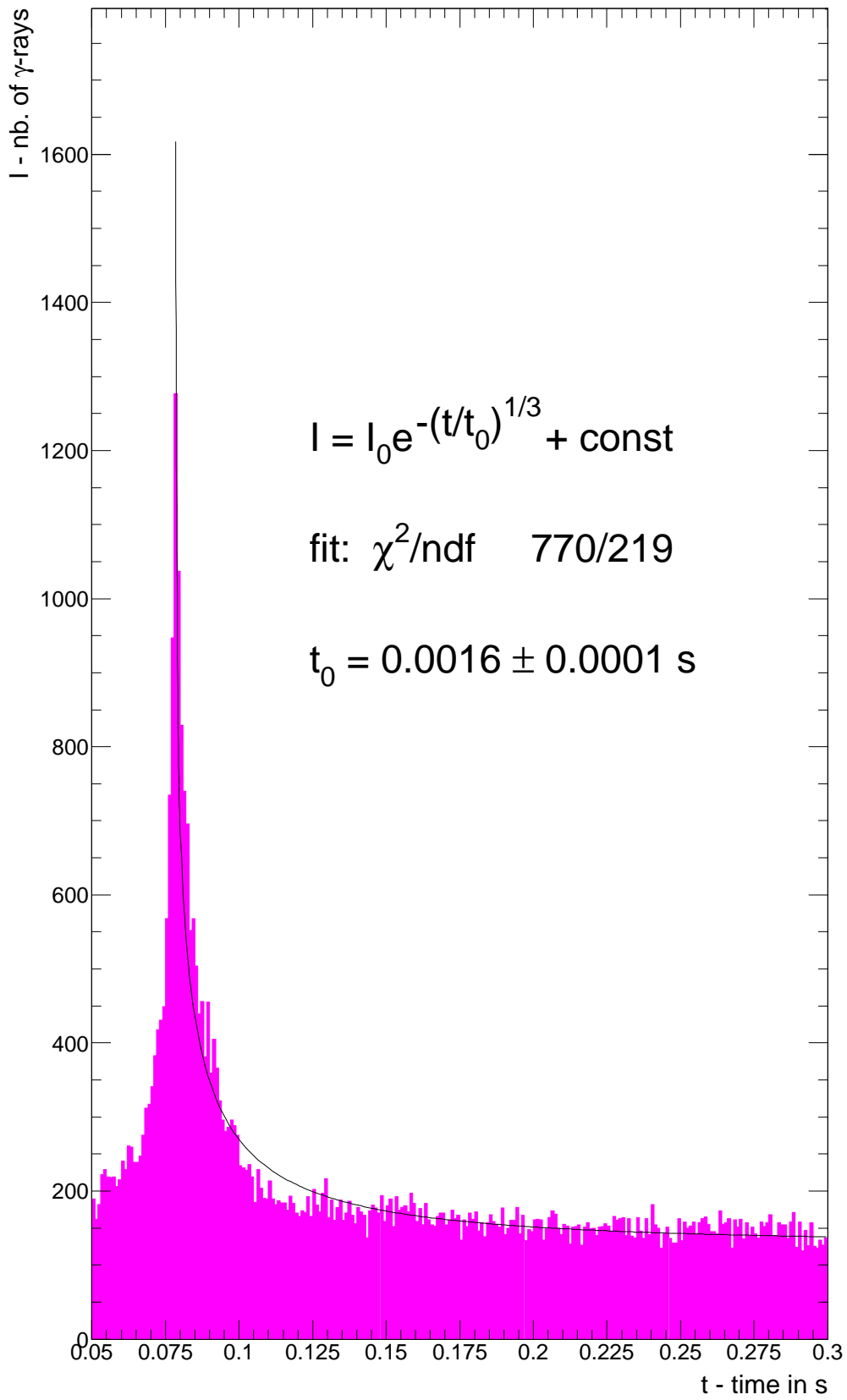


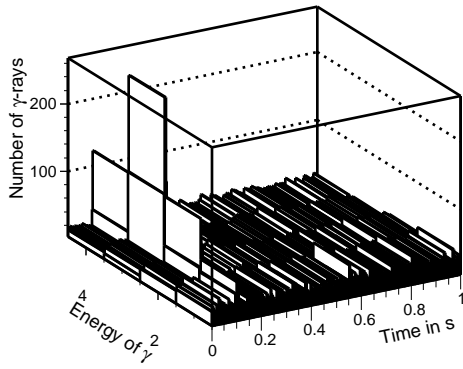
Trigger nr 3037



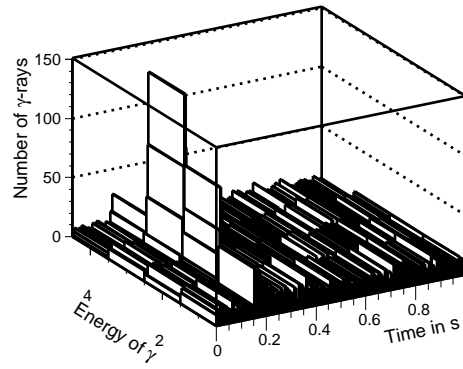
Trigger nr 2132



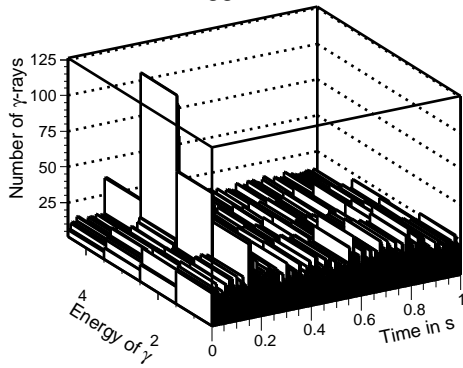




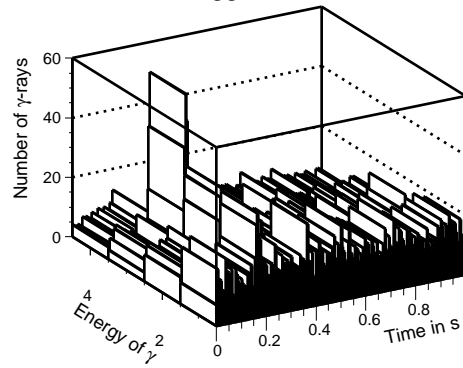
Trigger nr 0512



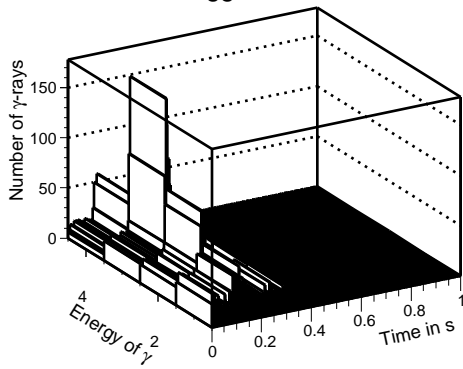
Trigger nr 1649



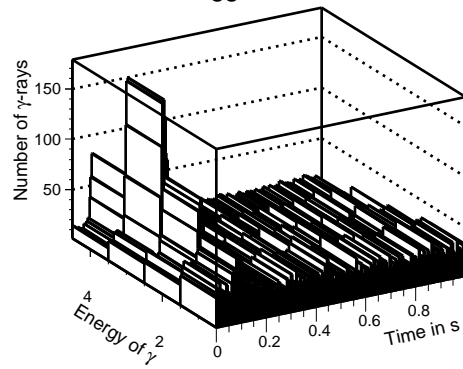
Trigger nr 0207



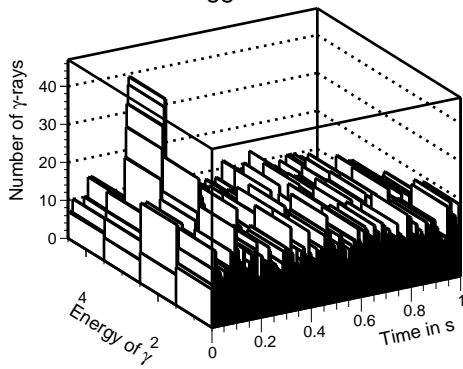
Trigger nr 2615



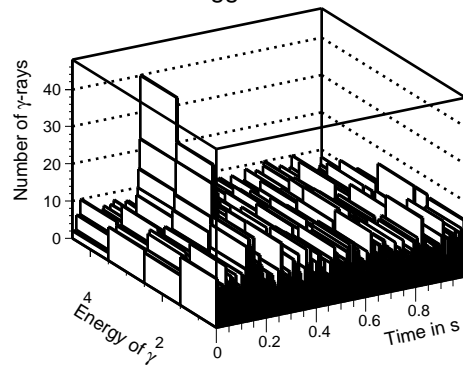
Trigger nr 0432



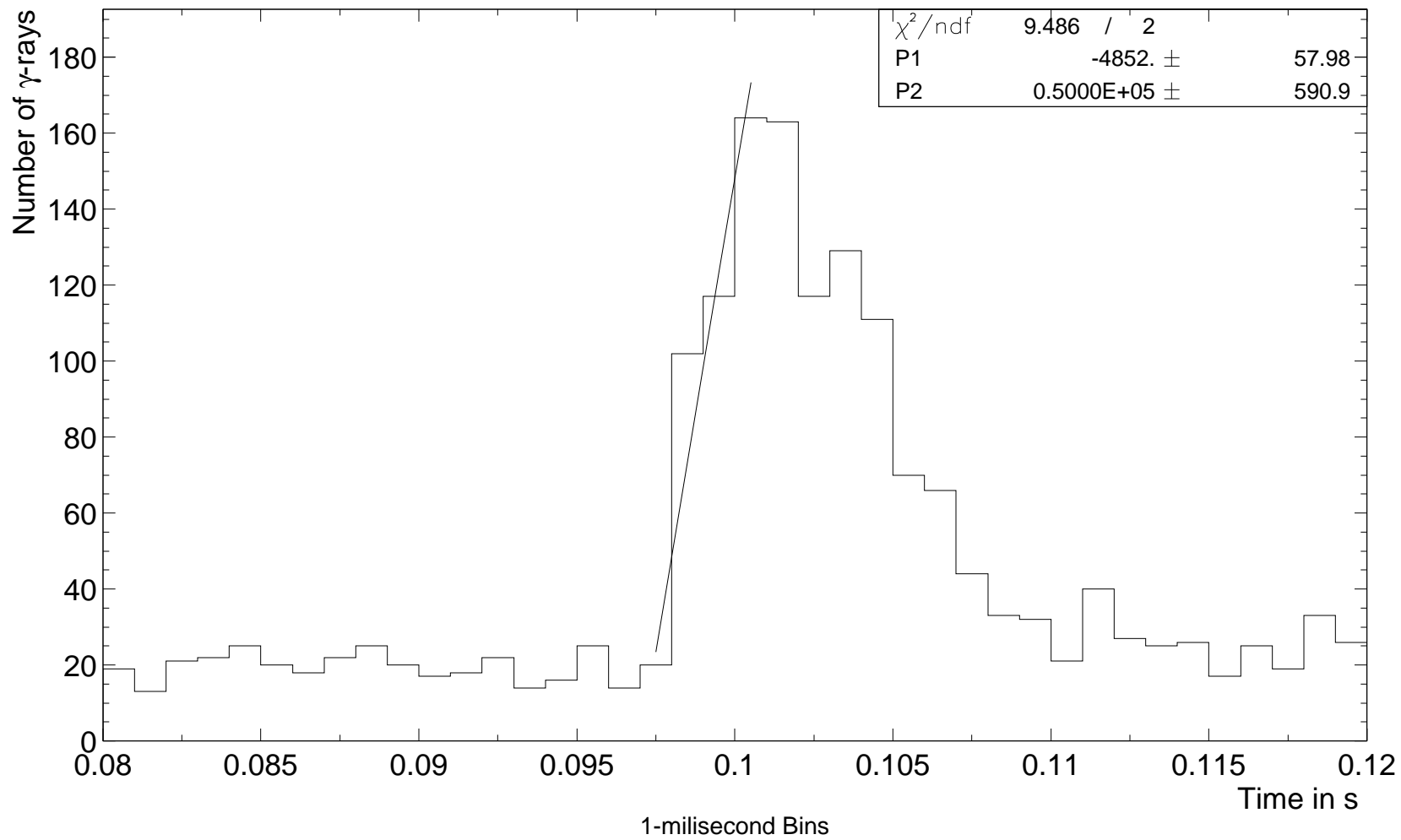
Trigger nr 0480

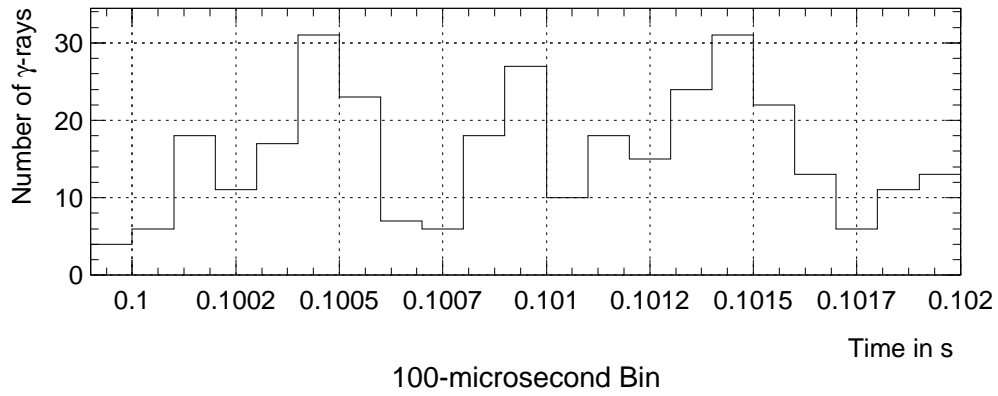
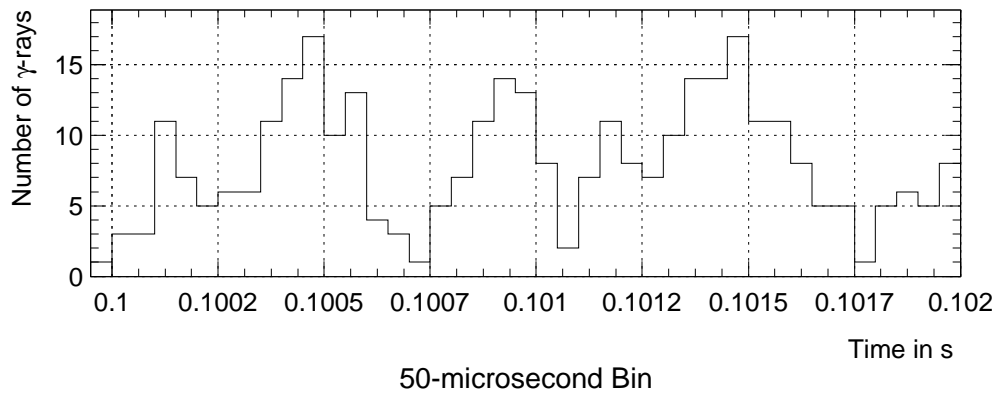
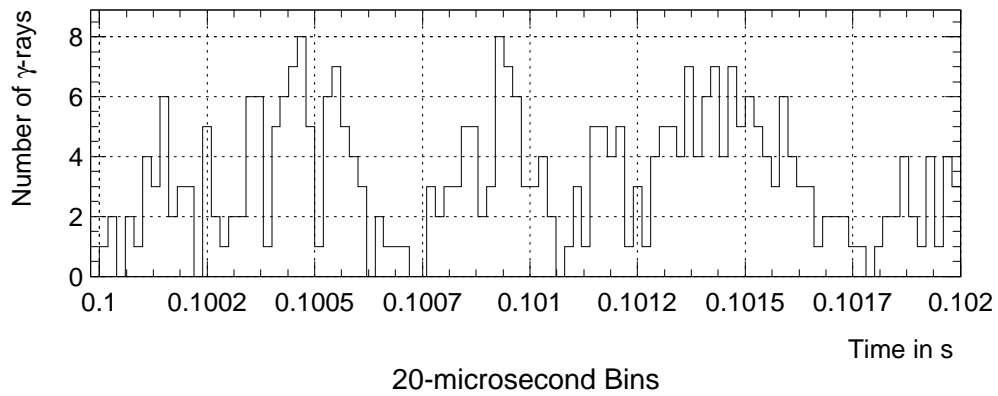
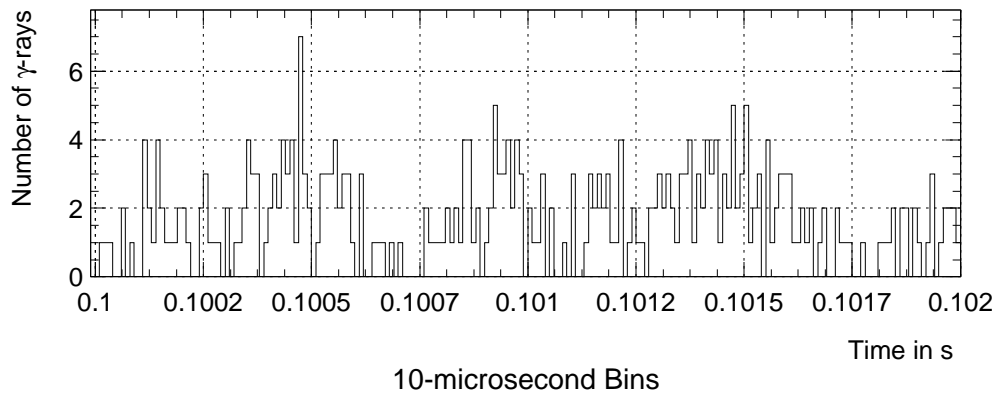


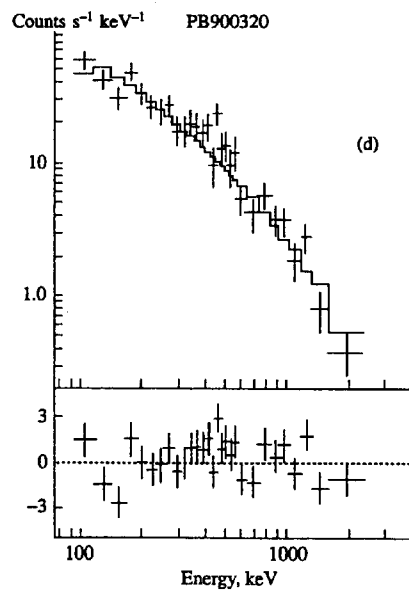
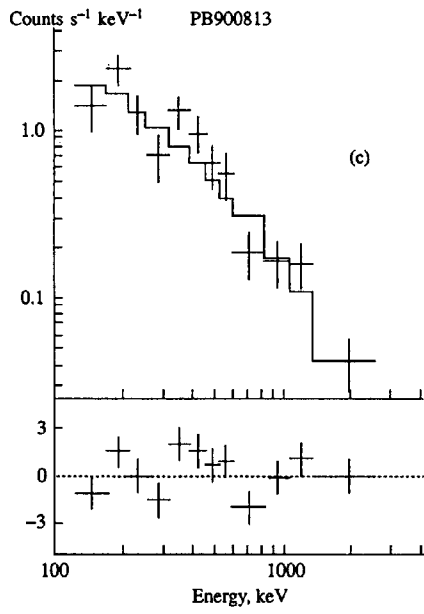
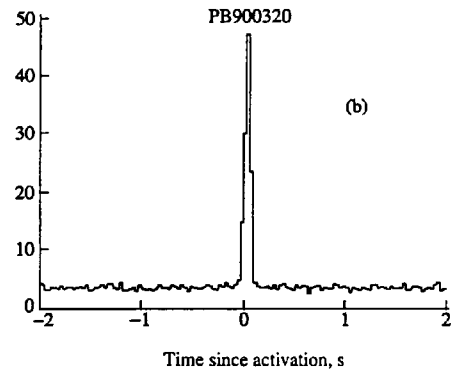
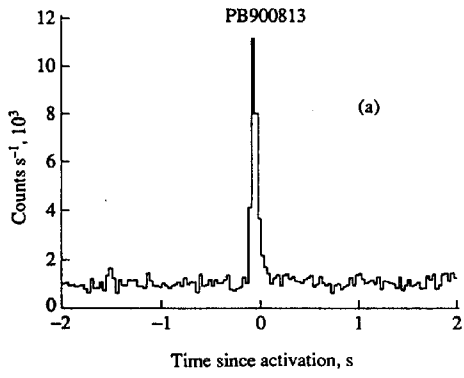
Trigger nr 3037

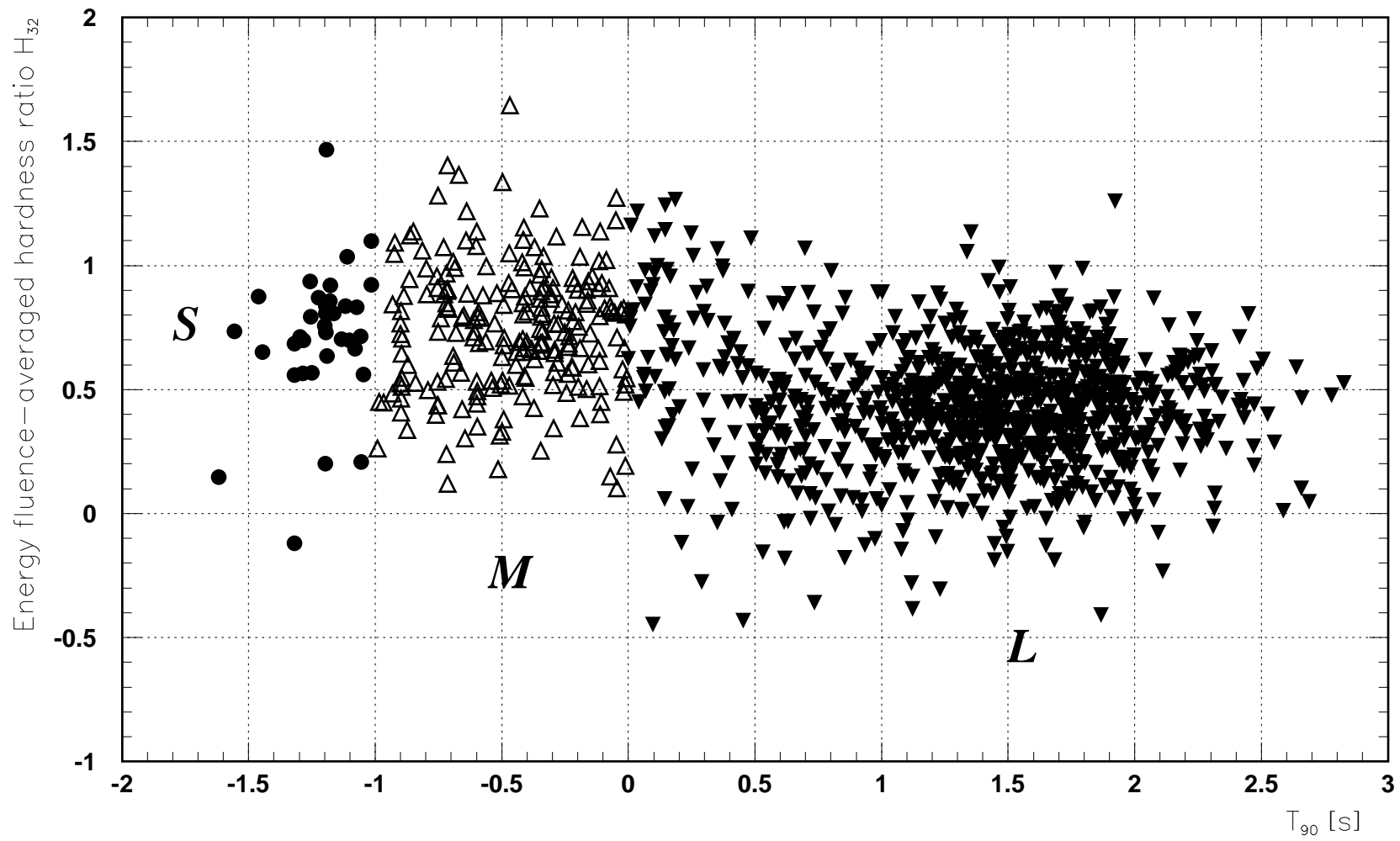


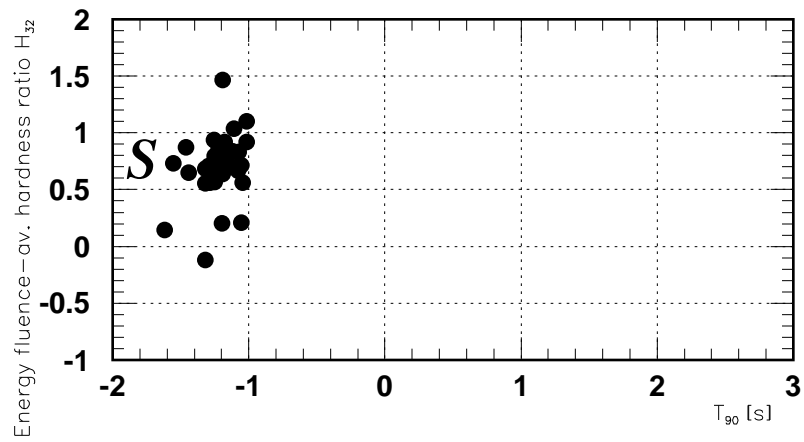
Trigger nr 2132



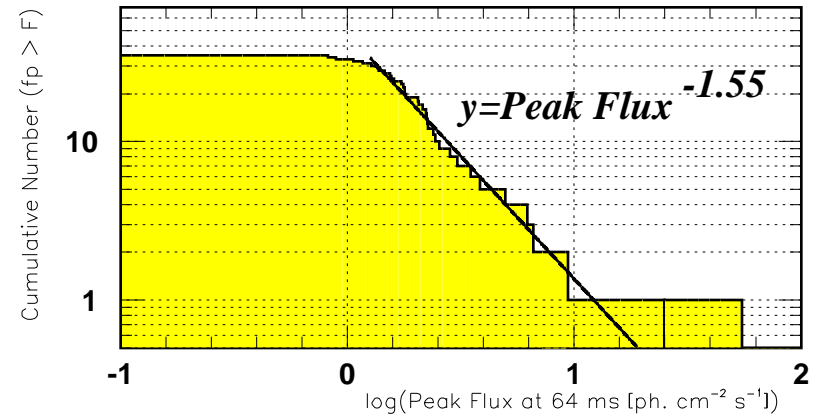




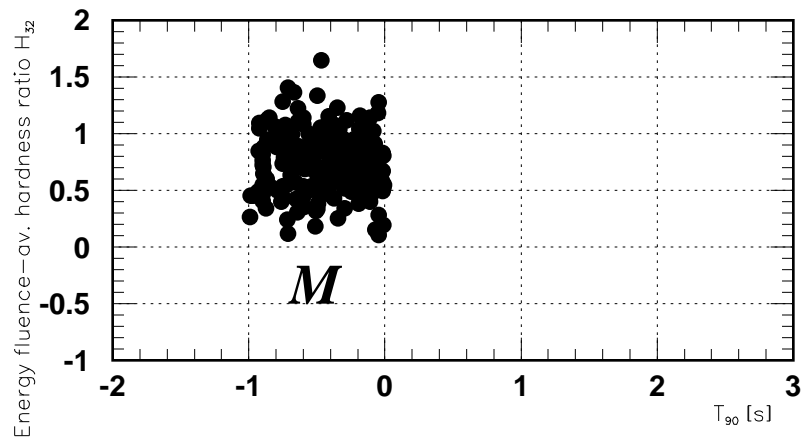




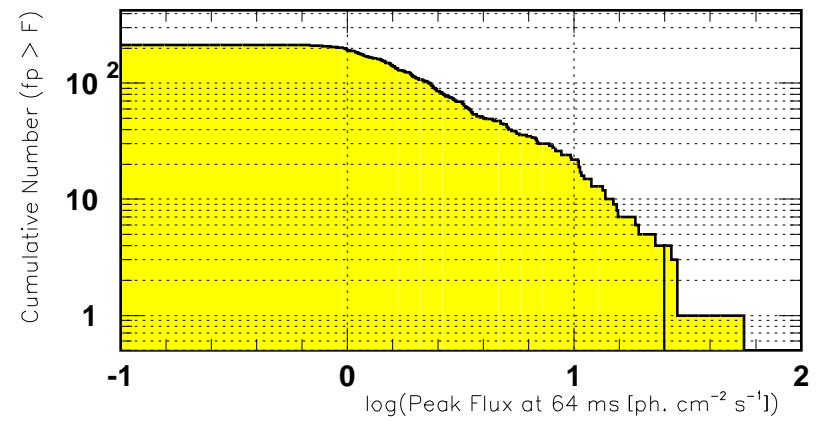
PLOT $\text{LOG}(T_{90}[\text{s}]) < -1.0$



CUMUL $\text{LOG}(T_{90}[\text{s}]) < -1.0 \text{ s}$



PLOT $-1.0 > \text{LOG}(T_{90}[\text{s}]) > 0.0$



CUMUL $-1.0 > \text{LOG}(T_{90}[\text{s}]) > 0.0$